#### S1 Finite-element mesh and resolution tests

The finite-element mesh is presented in Fig. S1 at transition and localization times  $t_{\rm tr}$  and  $t_{\rm PB}$  for the localizing simulation *ref-1*. In this simulation, the minimum element size allowed is either 1000 m and the maximum element size is 5 km for depth shallower than 100 km, or 100 km for the rest of the domain. The mesh auto-adaptivity criteria are set on temperature (5 K), velocity (3  $10^{-11}$  m s<sup>-1</sup>), strain rate ( $\log_{10}$  scale - 0.01) and viscosity ( $\log_{10}$  scale - 0.01). The latter two criteria are evidenced by the small element size at mid-lithospheric depths (viscosity increase), around the plate boundary and in the asthenosphere where flow diverges.

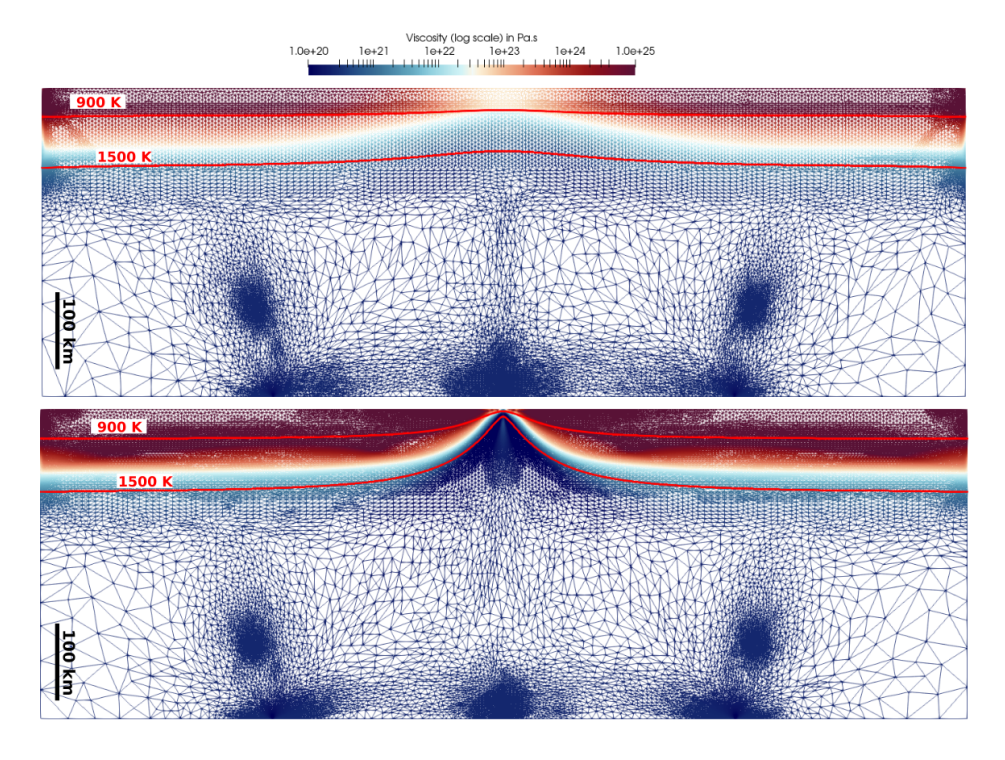


Figure S1. Finite-element mesh of the whole domain  $(1200 \times 40 \text{ km})$  superimposed on the viscosity field for Simulation *ref-1* (rheology  $D - d_{\text{LT-HT}} - Y_{500 \text{ MPa}}$ , initial plate age of 50 Myrs, extension rate  $v_{1/2}$  of 1 cm/yr) at the transition time  $t_{\text{tr}} = 6.5$  Myr (top), and at the time  $t_{\text{PB}} = 12$  Myr when the plate boundary becomes steady (bottom), similarly to the snapshots of Fig.3b in the main text.

We perform resolutions tests with the same adaptivity criteria, allowing minimum element sizes of 2000, 1000, 500, 200 or 100 m. For rheology  $D - d_{\rm LT-HT} - Y_{\rm 500~MPa}$ , deformation localization is slightly faster for smaller minimum edge lengths (Fig. S2a), however the time difference remains smaller than 1.5 Myr when increasing resolution from 1000 to 200 m. Thus, we choose 1000 m for minimum element size for most simulations in this study to allow reasonable computation times.

However, for when the yield-stress rheology is restricted to low temperatures  $(D-d-Y_{200/500\,\mathrm{MPa}}^{900/950K})$ , we observe a much larger difference between 1000 and 500 m (Fig. S2b). We explain this discrepancy by the issue of vertically resolving the high-viscosity layer at the transition between creep and yielding domain, which is only a few kilometers thick (Fig. 9a and c). These simulations are performed with a minimum element size of 200 m to ensure that the slow localization (described in Section 4.3 of the main text) is not mesh-dependent.

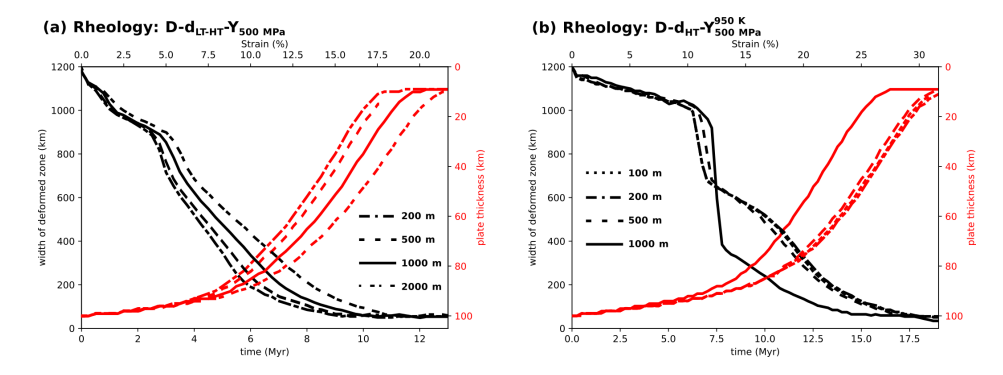


Figure S2. Influence of the mesh minimum element size on the width of the deformed zone w(t) (black lines) and on plate thickness  $h_{plate}$  at the domain center (red lines) for the reference setup (half-spreading rate  $v_{1/2}$  of 1 cm yr<sup>-1</sup> and initial plate age equal to 50 Myr). (a) Rheology  $D - d_{LT-HT} - Y_{500 \, MPa}$  combining diffusion creep, low- and high-temperature dislocation creep and a yield stress of 500 MPa. Transition and localization times  $t_{tr}$  and  $t_{PB}$  are of 6 Myr (resp. 6 or 6.5 Myr) and 10.5 (resp. 10.75 or 12 Myr) for minimum element mesh size of 200 m (resp. 500 or 1000 m). (b) Rheology  $D - d_{HT} - Y_{500 \, MPa}^{950 \, K}$  combining diffusion creep, high-temperature dislocation creep and a yield stress of 500 MPa restricted to temperatures lower than 950 K. Transition and localization times  $t_{tr}$  and  $t_{PB}$  are of 12.5 Myr (resp. 12.5, 11.75 or 8 Myr) and 19 Myr (resp. 19, 18.5 or 16 Myr) for minimum element mesh size of 100 m (resp. 200, 500 or 1000 m).

### S2 Outflow lateral boundary condition

The velocity outflow boundary conditions are calculated from a Couette flow applied to a diffusion creep viscosity profile for a plate of 50 Myr (Appendix A). The vertical velocity V(z) (Eq. A3) is a 10-th order polynomial ( $V(z) = c_{10} \cdot z^{10} + \cdots + c_1 \cdot z + c_0$ ), which coefficients are given in Table S1 for  $v_{1/2} = 1$  cm yr<sup>-1</sup>.

**Table S1.** Polynomial coefficients for  $v_{1/2} = 1$  cm yr<sup>-1</sup>. For other extension velocities, these coefficients are multiplied by a relative factor.

ĺ	$c_{10}$	<i>C</i> 9	$c_8$	<i>C</i> 7	$c_6$	$c_5$
Ì	$1.62607080 \ 10^{-63}$	$-4.53868567 \ 10^{-57}$	$5.60944110 \ 10^{-51}$	$-4.03504583 \ 10^{-45}$	$1.86626092 \ 10^{-39}$	$-5.77967776 \ 10^{-34}$
ĺ	$c_4$	$c_3$	$c_2$	$c_1$	$c_0$	
	$1.20780239 \ 10^{-28}$	$-1.66874438 \ 10^{-23}$	$1.43959164 \ 10^{-18}$	$-6.94070902\ 10^{-14}$	$1.73487485 \ 10^{-9}$	

In all the numerical experiments described in the main text, the prescribed velocity at the lateral boundaries is calculated for a plate of 50 Myr (Appendix A), which we term 'Couette age' - even if the actual initial thermal plate age of the simulation is different (e.g. 10 Myr or 100 Myr). We run additional simulations at  $v_{1/2} = 1$  cm yr $^{-1}$  with the velocity 'Couette age' identical to the initial thermal age of 10 (resp. 100 Myr),resulting in a thinner (resp. thicker) 'constant velocity' outflow than with a 50 Myr 'Couette age'. We only note a slightly faster localization ( $\sim$ 0.5 Myr) when the 'Couette' age is larger than the 'thermal' age (Fig. S3).

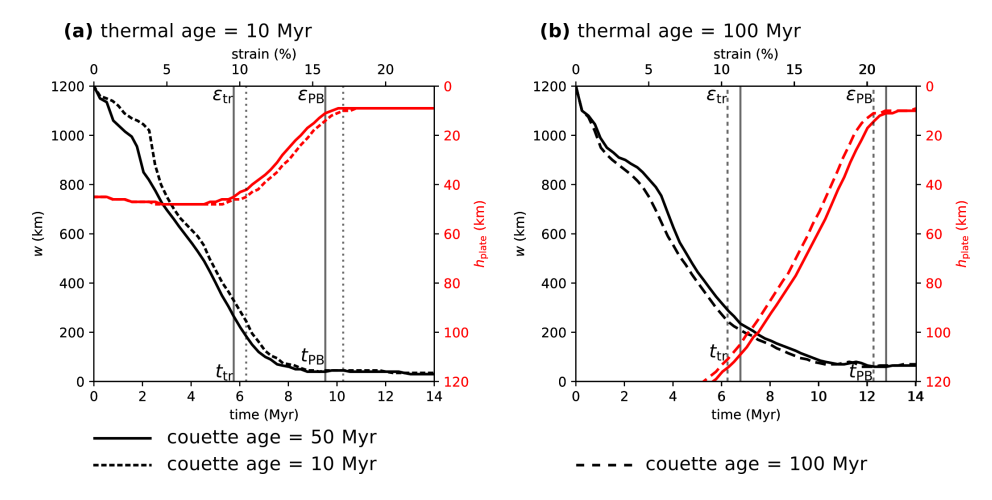
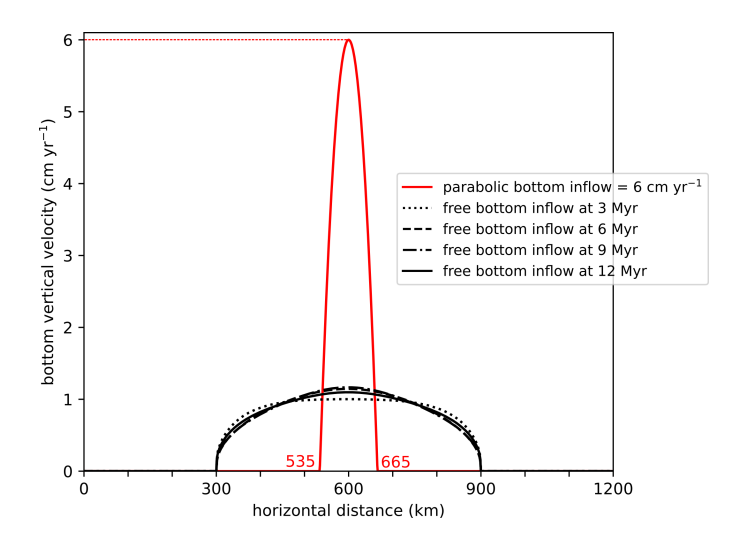


Figure S3. Evolution of the width of the highly deforming zone w(t) (black), and of the plate thickness  $h_{plate}(t)$  (red) for  $v_{1/2} = 1$  cm yr<sup>-1</sup>, for initial 'thermal' plate ages of 10 Myr (a) or 100 Myr (b). Dashed and solid compare results for 'Couette' age (boundary condition of the lateral velocity profiles) either identical to the thermal age, or of 50 Myr).

### S3 Inflow at the bottom boundary

The default bottom boundary conditions enables a purely vertical free flow over a 600-km wide, adjusting to the imposed horizontal lateral and the free-surface deformation, with steady maximum velocities slightly greater than 1 cm yr<sup>-1</sup> for  $v_{1/2}$  of 1 cm yr<sup>-1</sup> (Fig. S4). For the simulation with an imposed vertical inflow (Appendix B), the central maximum velocity if set to 6 cm yr<sup>-1</sup> over a 130-km wide segment (Fig. S4).



**Figure S4.** Vertical velocity along domain bottom at different times during Simulation *ref-1* (black lines), or imposed as a parabolic inflow for the simulation described in Appendix B.

## S4 Calculation of plateness P(t)

Plateness is a measure of how much surface deformation is spatially localized in narrow boundaries (Tackley, 2000; Crameri, 2018; Fuchs and Becker, 2019), defined as:

35 
$$P = 1 - \frac{f_{80}}{f_c}$$
 (S1)

where  $f_c$  is a relative reference surface (or distance) ( $f_c = 1$  here) and  $f_{80}$  is a relative fraction of the total surface (or distance) in which 80 % of the cumulative deformation occurs (see Fig. S5, for 2-D calculation using relative distance).

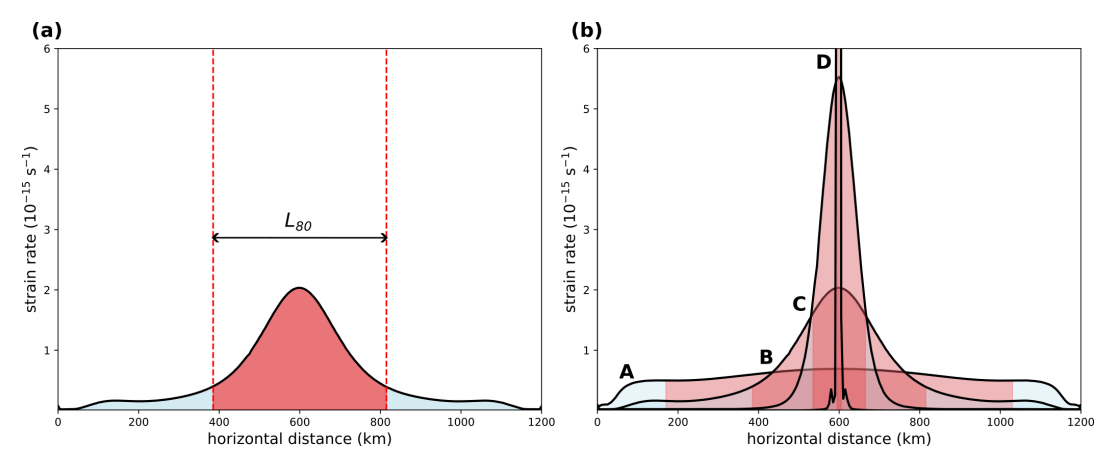


Figure S5. (a) Calculation of plateness P: lateral profile of the strain rate second invariant at the box surface in Simulation *ref-1* at 5 Myr. The cumulative deformation is represented by the sum of grey and red areas.  $L_{80}$  is the distance over which the 80 % of the cumulative deformation occurs (red area). Fraction  $f_{80} = L_{80}/L$ , where L is the width of the simulation box (1200 km). (b) Strain rate lateral profiles at times 1 Myr (A) - resp. 5 Myr,  $t_{tr} \sim$ 6.5 Myr (C),  $t_{PB} \sim$ 12 Myr (D) - with peak peak strain rate of 0.67 (resp. 2.0, 5.5, 117)  $10^{-15}$  s<sup>-1</sup> and fraction  $f_{80}$  of 0.72 (resp. 0.36, 0.11, 0.01).

# References

- Crameri, F.: Geodynamic diagnostics, scientific visualisation and StagLab 3.0, Geoscientific Model Development, 11, 2541–2562, https://doi.org/10.5194/gmd-11-2541-2018, 2018.
  - Fuchs, L. and Becker, T. W.: Role of strain-dependent weakening memory on the style of mantle convection and plate boundary stability, Geophysical Journal International, 218, 601–618, publisher: Oxford University Press, 2019.
- Tackley, P. J.: Self-consistent generation of tectonic plates in time-dependent, three-dimensional mantle convection simulations 2. Strain weakening and asthenosphere, Geochemistry, Geophysics, Geosystems, 1, https://doi.org/10.1029/2000GC000043, \_eprint: https://onlinelibrary.wiley.com/doi/pdf/10.1029/2000GC000043, 2000.